

RESEARCH ARTICLE

10.1029/2022JA031078

Key Points:

- Significant intensity enhancements at frequencies of 1.5–4 kHz occur at Kannuslehto mainly on the dawn side and last for several hours
- Simultaneous observations by Van Allen Probes reveal that the waves are likely dawn side whistler mode chorus
- Unducted propagation to the ground requires equatorial wave normals much larger than observed, indicating the importance of wave ducting

Correspondence to:

B. Bezděková,
barbora.bezdekova@mff.cuni.cz

Citation:

Bezděková, B., Němec, F., Manninen, J., Santolík, O., Hospodarsky, G. B., & Kurth, W. S. (2023). Very low frequency whistler mode wave events observed simultaneously by the Kannuslehto station and Van Allen Probes. *Journal of Geophysical Research: Space Physics*, 128, e2022JA031078. <https://doi.org/10.1029/2022JA031078>

Received 12 OCT 2022

Accepted 29 DEC 2022

Very Low Frequency Whistler Mode Wave Events Observed Simultaneously by the Kannuslehto Station and Van Allen Probes

B. Bezděková¹, F. Němec¹, J. Manninen², O. Santolík^{1,3}, G. B. Hospodarsky⁴, and W. S. Kurth⁴

¹Faculty of Mathematics and Physics, Charles University, Prague, Czech Republic, ²Sodankylä Geophysical Observatory, Sodankylä, Finland, ³Department of Space Physics, Institute of Atmospheric Physics of the Czech Academy of Sciences, Prague, Czech Republic, ⁴Department of Physics and Astronomy, University of Iowa, Iowa City, IA, USA

Abstract Events characterized by substantial intensity enhancements in the frequency range between about 1.5 and 4 kHz in the measurements of the ground-based Kannuslehto station, Finland are analyzed. Altogether, as many as 465 events are identified in the Kannuslehto data measured during the campaigns between December 2012 and October 2019. It is shown that the events usually last for several hours and they occur preferentially on the dawn side during geomagnetically active periods. Simultaneous measurements performed by the Van Allen Probes spacecraft are used to reveal the L -shells and magnetic local times where a corresponding intensity increase occurs in space. A backward ray tracing analysis is further employed to investigate the wave propagation between the tentative source region and the ground. Wave normal angles of waves eventually detectable at Kannuslehto are determined and compared with those obtained from a detailed wave analysis. Either a wave ducting, propagation in the Earth-ionosphere waveguide, or their combination seem to be needed for the waves to reach Kannuslehto.

1. Introduction

Measurements of very low frequency (VLF) whistler mode waves represent one of the main tools for studying processes in the Earth's inner magnetosphere. Due to the relatively straightforward measurement technique used for their detection, they have been studied on the ground for more than 60 years (Helliwell, 1965). However, while their detection provides a remarkable amount of information about the magnetosphere, generation mechanisms, properties, and means of propagation of many of the observed wave phenomena are not yet fully understood (e.g., Bezděková et al., 2019; Breuillard et al., 2014; Green et al., 2005; Manninen, 2005; Rodger et al., 2000). Hence, they are still in the scope of intense research.

Waves reaching a ground-based station either originate directly near the Earth or they propagate toward the Earth from the magnetosphere. In the first case, they are usually a result of the lightning activity near the station or are of anthropogenic origin; in the latter case, their wave vectors have to be suitably oriented to penetrate through the ionosphere and eventually reach the ground (Helliwell, 1965). Due to the sudden change of the refractive index at the bottom of the ionosphere, incident whistler mode wave vectors have to be oriented nearly vertically down in order not to be reflected back. Upon penetration through the ionosphere, the waves can propagate substantial distances in the Earth-ionosphere waveguide (Budden, 1961) before eventually reaching the receiver station. A significant wave attenuation in the ionosphere, in particular during the daytime (Cohen et al., 2012), along with relatively strict conditions for the waves to reach the ground are the reason that only their small fraction is eventually detected by ground-based instruments (e.g., Graf et al., 2013; Sonwalkar, 1995).

A powerful tool for the wave propagation analysis is a comparison of simultaneous measurements, best provided by a ground-based station and a spacecraft. In such a case, it is possible to study both the temporal and spatial evolution of the waves (e.g., Martínez-Calderon, Němec, et al., 2020; Titova et al., 2015) and to obtain important pieces of information about the wave propagation (Demekhov et al., 2021; Martínez-Calderon et al., 2016). Moreover, statistical studies of such wave events can provide an overall picture of the favorable conditions for the wave occurrence and penetration through the ionosphere. However, it is challenging to obtain a sufficiently large data set to perform such a statistical analysis, and hence only case studies are often reported (e.g., Demekhov et al., 2017, 2021; Martínez-Calderon, Katoh, et al., 2020; Němec et al., 2016). These case studies focus on a

concrete kind of whistler mode waves, quasiperiodic emissions (Carson et al., 1965; Sato & Kokubun, 1980), and a detailed analysis of available multipoint observations.

Recent examples of case studies focused on a comparison of whistler mode wave measurements performed simultaneously by a ground-based station and a spacecraft were presented, for example, by Santolík et al. (2009), Jaynes et al. (2015), Demekhov et al. (2017, 2020), and Martinez-Calderon, Katoh, et al. (2020). These works are often motivated by searching for a possible source region of the waves and their exact propagation toward the ground. Additionally, a possible connection of the detected wave events with other simultaneously observed phenomena, such as Pc4–5 ULF waves (Menk, 2011), is discussed. Statistical studies of this kind were performed, for example, by Ma et al. (2017) and Bezděková et al. (2020). The statistical study performed by Ma et al. (2017) is focused on the Van Allen Probes observations of VLF waves emitted by ground-based transmitters between 2012 and 2016. Bezděková et al. (2020) discuss conjugate observations of quasiperiodic emissions by the Kannuslehto station and the Van Allen Probes spacecraft between September 2012 and November 2017.

Sometimes more instruments than two detect the same emissions, which can naturally lead to a more comprehensive study. An analysis of periodic VLF emissions detected simultaneously by the Van Allen Probes spacecraft and two ground-based stations, Kannuslehto and Lovozero, was presented by Demekhov et al. (2021). An event detected in March 2019 with wave normal angles measured by Van Allen Probes below 40° for the whole duration was analyzed. The event duration as observed by Kannuslehto was about 1.5 hr, and its propagation was described in detail, including an analysis of individual event pulse periods and their connection with the waves traveling in the magnetosphere. The event generation was linked to the cyclotron maser (e.g., Bespalov et al., 2010; Trakhtengerts & Rycroft, 2008).

Martinez-Calderon, Katoh, et al. (2021) studied properties of several types of VLF waves observed simultaneously by the Kannuslehto station and Arase spacecraft. Altogether, 13 conjugate events found during the Kannuslehto 2017–2018 campaign were analyzed. Most of the events were classified as quasiperiodic emissions. The events lasted from several minutes to 3 hr, and they usually took place during the afternoon. Moreover, they were observed during rather quiet geomagnetic conditions and the wave normal angles observed by Arase were larger than 20° . The mechanism for how the waves can reach the Kannuslehto station was discussed, indicating that the waves typically propagate unducted and reach the ground southwards from Kannuslehto, usually around the same position.

Manninen et al. (2021) and Manninen et al. (2022) reported a new type of VLF whistler mode wave found in the Kannuslehto station measurements. The events, so-called “VLF birds” and “VLF bursty-patches,” occur at frequencies above 4 kHz, and they emerge in frequency-time spectrograms only after filtering out strong emissions of lightning origin (sferics) occurring in the same frequency range. The emissions are observed under rather quiet geomagnetic conditions, last for a few hours, and have a form of a sequence of short (~few minutes long) structures. A peculiar fact about these emissions is that they occur at frequencies above the equatorial electron cyclotron frequency corresponding to the Kannuslehto *L*-shell (~ 2.7 kHz). The question how these events are generated and how they propagate to Kannuslehto remains unanswered. However, a former conjugate ground-spacecraft observation of one such event (Titova et al., 2017) indicates their probable generation at sufficiently low *L*-shells and with subsequent propagation in the Earth-ionosphere waveguide.

The present paper is focused on the analysis of VLF whistler mode wave events at frequencies between about 1.5 and 4 kHz characterized by intensity enhancement with various structures in frequency-time spectrograms measured by the Kannuslehto station, Finland. The chosen frequency range corresponds to the most visible intensity enhancements which can be clearly identified and their beginning and ending times quite unambiguously determined (see further). The measurements are compared with the Van Allen Probes spacecraft data and possible source locations of the events in the equatorial region at larger distances are determined. A backward ray tracing analysis is further used to analyze the wave propagation between the tentative source region and the ground.

Both the ground-based station Kannuslehto and the Van Allen probes spacecraft mission are introduced in Section 2. The procedure of identifying the events and some examples are also described in Section 2. Section 3 contains description of the obtained results, which are discussed in Section 4. Main results are summarized in Section 5.

2. Data Set

In this study, VLF wave measurements of the Finnish Kannuslehto station and two Van Allen Probes (abbreviated as RBSP according to their original name Radiation Belt Storm Probes) spacecraft are analyzed. Data covering the entire RBSP mission (from August 2012 to October 2019) are used. Considering the lengths of individual Kannuslehto campaigns in this period, this corresponds to more than 1,000 days of simultaneous measurements by all instruments.

The Kannuslehto station, Finland is situated at 67.74°N, 26.27°E, corresponding to L -shell of about 5.53. The station is managed by Sodankylä Geophysical Observatory (SGO) in Sodankylä. Measurements at the Kannuslehto station are provided by two magnetic loop antennas of effective areas of 1,000 m² (both with size 10 × 10 m and with 10 turns) oriented in the geographical north-south and east-west directions. They supply wave measurements in the frequency range 0.2–39 kHz. Data are sampled with the sampling rate 78,125 Hz, exhibit a wide dynamic range (up to 120 dB) and an extraordinary sensitivity ($\sim 10^{-14}$ nT²Hz⁻¹). Due to technical reasons, partly related to significant lightning emissions during summer, the station typically operates in campaigns lasting for several months from autumn to spring. Altogether, eight Kannuslehto campaigns took place during the RBSP mission duration. These correspond to more than 1,000 measurement days when the RBSP spacecraft data are available.

The Van Allen Probes mission consisted of two spacecraft (A, B) which operated from August 2012 to either July 2019 (RBSP B) or October 2019 (RBSP A). These satellites had nearly identical elliptical orbits close to the equatorial plane, covering radial distances from about 1.1 R_E to 5.8 R_E . The corresponding range of L -shells was between about 1.1 and 6.5. All magnetic local times (MLTs) and geomagnetic longitudes were sampled during the course of the mission. Multicomponent wave measurements in the frequency range 10 Hz–12 kHz were performed by the instrument suite EMFISIS (Electric and Magnetic Field Instrument Suite and Integrated Science), see Kletzing et al. (2013). The EMFISIS Waves instrument supplied measurements of three magnetic and three electric field components. In the present study, the survey mode data are used, where the analyzed frequency interval is divided into 64 quasi-logarithmically organized channels based on a 0.5 s waveform captured every 6 s. A variety of other additional parameters allowing one to better understand the wave propagation were calculated from the obtained data. Parameters such as planarity, ellipticity, wave and Poynting vectors were derived via standardized routines (Santolík et al., 2002, 2003, 2010).

In this study, we aim to analyze emissions detected simultaneously by a ground-based instrument and at least one RBSP spacecraft to better understand their propagation. For this purpose, we focused exclusively on the time intervals when the Kannuslehto station detected a clear intensity enhancement, visually identifiable in a corresponding frequency-time spectrogram. No particular frequency-time structure of the events was assumed. However, the investigation of the 24 hr long frequency-time spectrograms measured at Kannuslehto revealed frequent dawn side intensity enhancements in the frequency range from around 1 to 4 kHz. Such intensity variations were included in the present analysis if they were sufficiently isolated to clearly determine both their beginning and ending times and they occurred in the frequency range above 1 kHz. It was often not possible to meet these conditions for events detected on the dusk side due to substantial intensity enhancements through the whole frequency range for basically all night hours. Since it was typically not clear at which frequencies the emission occurs and how intensive it is, these emissions were not included in the list. Altogether, 465 such events were found in Kannuslehto data between December 2012 and October 2019. Notice that the character of such defined emissions sometimes varies considerably.

Examples of two identified events are shown in Figure 1. Figure 1a shows an event detected on 10 January 2014 between around 2:00 UT and 7:00 UT in the frequency range from about 2 to 3.5 kHz. No inner structure is apparent and solely the intensity enhancement characterizes the event. In contrast, the event depicted in Figure 1b which occurred on 20 November 2017 between about 0:00 UT and 6:30 UT at frequencies around 2 kHz is a QP event with evident inner structure. Moreover, there is an additional event appearing between around 2:00 UT and 5:00 UT at frequencies around 1 kHz.

Having presented some illustrative events identified according to the given criteria in the Kannuslehto data, let us briefly explain the reason for these criteria. As can be seen in the average spectrogram (in terms of magnetic local time, MLT) in Figure 2, there are several characteristic increases of the wave intensities. There are evident lightning related intensity enhancements at higher frequencies during night hours (Záhlava et al., 2018, 2019) and

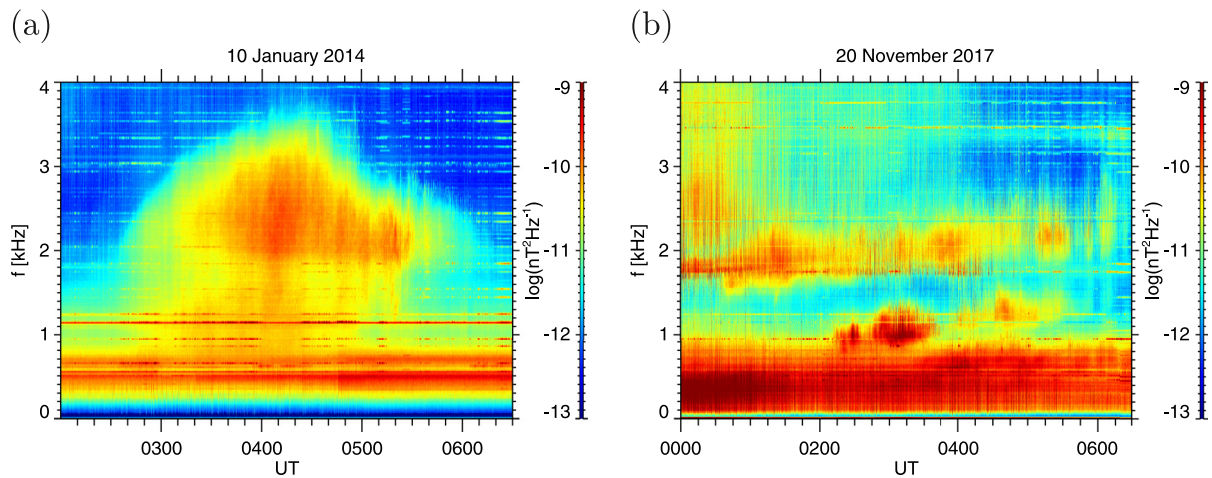


Figure 1. Spectrograms of two events observed by the Kannuslehto station (a) on 10 January 2014 between around 2:00 UT and 7:00 UT in the frequency range from about 2 to 3.5 kHz and (b) on 20 November 2017 between 0:00 UT and 6:30 UT at frequencies around 2 kHz. Notice also an additional event in panel (b) occurring between around 2:00 UT and 5:00 UT at frequencies around 1 kHz.

substantial hiss wave activity at frequencies up to 1 kHz for the whole day (e.g., Aryan et al., 2021). However, at times, there is also a daytime intensity increase at frequencies between about 1 and 4 kHz. Due to their frequency-time confinement, these emissions can be unambiguously defined and distinguished. Moreover, the average intensity spectrogram in Figure 2 indicates that such emissions are quite intense and occur regularly, being of a possible global importance.

3. Results

At first, we attempt to characterize basic properties of the identified Kannuslehto events. Figure 3a shows a histogram of the duration of the events, while Figure 3b shows the number of events detected in individual 1 hr length MLT intervals. It can be seen that the events typically last for several hours, mostly up to about 10, but long lasting events are occasionally detected. Figure 3b reveals that the events indeed usually occur on the dayside, mostly between about 6 and 18 hr of MLT, with the peak occurrence during the morning period.

Characteristic geomagnetic conditions during the event observations are investigated in Figure 4. It shows a histogram of Kp indices detected at central times of the events by the black line. For comparison, a histogram of Kp indices during the entire Kannuslehto campaigns between 2012 and 2019 is shown by the red line. It can be seen that the Kp indices are slightly higher during the event occurrence (median values of Kp 1+ and 2-, respectively).

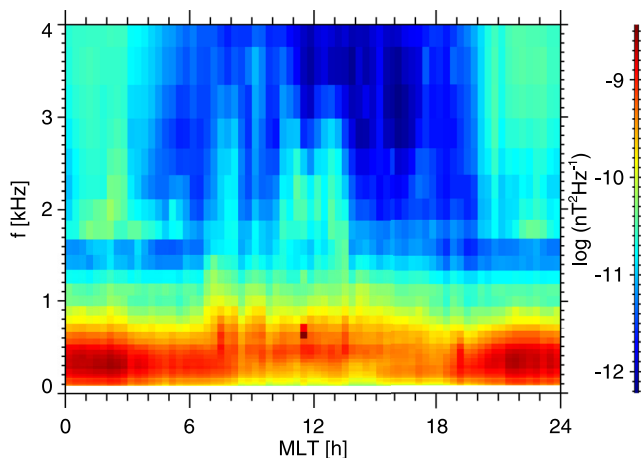


Figure 2. Average frequency-magnetic local time spectrogram of the wave intensities measured by the Kannuslehto station during campaigns between 2012 and 2019 in the frequency range between 0 and 4 kHz.

The compiled list of events further revealed that a considerable number of events occur immediately after each other for several days. This indicates that the actual event durations may be larger than observed, with the events only temporarily not being detected by Kannuslehto due to their limited extent in MLT. This is further analyzed in Figure 5. The blue line shows expected probabilities of events being observed for several consecutive days when assuming they are independent. The orange line shows the actually observed ratios of event durations in the data set. The sum of these fractions is thus equal to 100%. Due to the typically comparable MLTs of the event occurrences in all cases, it was solely analyzed whether the events occur in the several consecutive days, not at the same MLTs. It is apparent that the events tend to occur in consecutive days more often than would correspond to independent measurements, indicating that the actual event duration is often a couple of days.

The frequency spectrum of the events is analyzed in Figure 6. The average frequency spectrum at the times of the events is shown by the red curve,

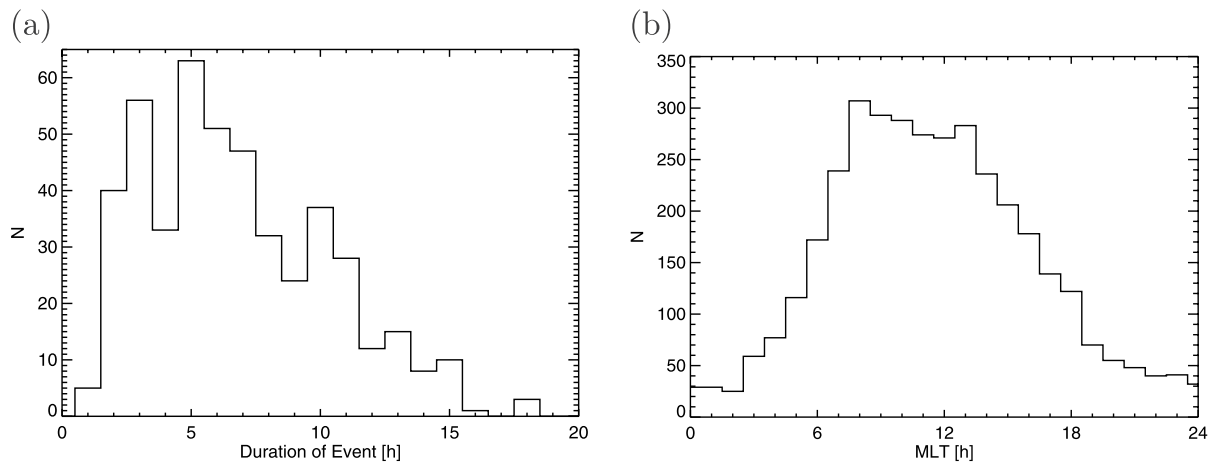


Figure 3. (a) Histogram of durations of the events detected at the Kannuslehto station. (b) Number of events detected in individual MLT intervals.

while the black curve shows the average frequency spectrum during all the analyzed Kannuslehto campaigns. Because emissions at higher frequencies were not considered in the present study, the spectra are depicted solely up to 5 kHz. It can be seen that the average intensities measured during the events are increased in comparison to the long-term average intensities, in particular at frequencies between around 1.5 and 4 kHz. This indicates a typical frequency range of the events. Note that the intensity increase during the event detection is comparatively weak, by a factor of 2 in power, 1.4 in amplitude. This is due to the fact that there was not any numerical criterion for the event identification and only a detectable intensity enhancement well confined in frequency and time was enough to include the event. Strong emissions lasting for a substantial time interval and spanning over a large frequency range which do not meet the given criteria for events thus contribute to the average spectrum and have comparable intensities.

In order to investigate how the emissions propagate before actually reaching the Earth, measurements performed by another instrument located between the Kannuslehto station and the source region are desirable. Moreover, if this other instrument is a spacecraft, one can take advantage of its movement and the fact that it typically covers a substantial region. In our case, RBSP measurements were employed, covering a wide range of L -shells and a complete range of MLTs. Results of this analysis are shown in Figure 7.

Figure 7 shows how the power spectral density of magnetic field fluctuations in the event frequency range (between 2 and 4 kHz) varies during the event observations as a function of MLT and L -shell. In Figure 7a, average values obtained for all RBSP A measurements during the whole mission are depicted. Figure 7b shows the same dependence, but only data measured during the times of the Kannuslehto events were considered. No requirement for the spatial conjunction with the Kannuslehto station is imposed. This provides an overall picture of magnetospheric wave intensities at the times of the events, indicating possible L -shell-MLT intervals close to the geomagnetic equator where the events eventually observed on the ground originate. In order to demonstrate the general effect of geomagnetic conditions, Figure 7c depicts the situation irrespective of the event occurrence, but at the times when K_p indices were larger than 5. Finally, Figure 7d shows the ratio of intensities from Figure 7b (during the events) and Figure 7a (long-term average). This plot gives better insight into in which MLT and L -shell bins the wave intensities increase during the events.

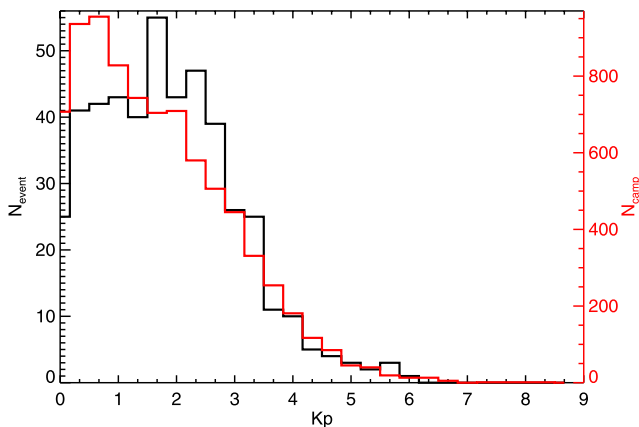


Figure 4. Histogram of K_p indices at the central times of the events (black line) and histogram of K_p indices during the entire Kannuslehto campaigns between 2012 and 2019 (red line).

Figures 7a–7c reveal there is a typical MLT– L -shell profile of significant wave intensities on the nightside, the intensity is the largest at L -shells around 2. The L -shell of the largest intensities is somewhat larger (≈ 3), and the intensities are lower during the day, with the overall picture being roughly symmetric around noon. The waves responsible for this intensity increase are

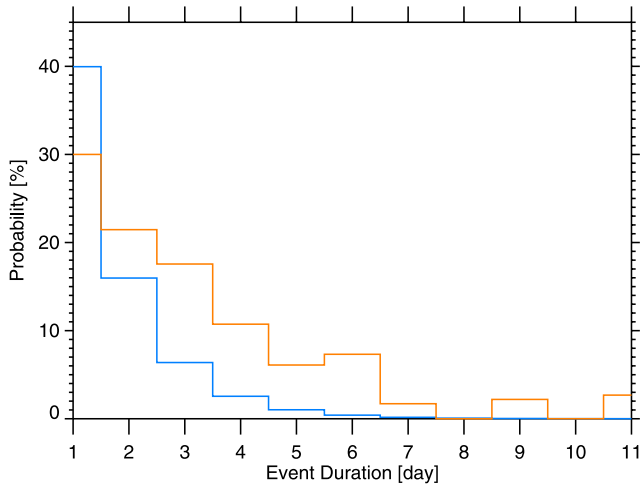


Figure 5. Probability of observing the event for several consecutive days. Expected probability if the measurements are independent (blue line) and the actually observed distribution (orange line).

believed to be primarily lightning generated whistlers (Němec et al., 2010; Záhlava et al., 2019). An additional MLT– L -shell region of significant wave intensities is observed on the dawn side at L -shells around 5, corresponding to chorus waves (Li et al., 2011). This MLT– L -shell interval corresponds to the interval of large relative intensity values in Figure 7d, suggesting that these are the waves forming the events identified in the Kannuslehto data. Note that the Kannuslehto station is located at L -shell ~ 5.5 , that is, it is at slightly larger L -shells than these candidate corresponding waves measured close to the equator.

Wave normal angle, which can be readily obtained from the multicomponent RBSP data (Santolík et al., 2003), is the parameter ultimately controlling the wave propagation. Its values at the times of the Kannuslehto events are shown in Figure 8. It depicts the probability density of the wave normal angle values in the frequency range between 2 and 4 kHz as a function of L -shell. Only the waves with power spectral densities of magnetic field fluctuations larger than $10^{-8.5} \text{ nT}^2 \text{ Hz}^{-1}$ and magnetic field planarities larger than 0.5 were included in the analysis, excluding thus a significant number of observations (see, e.g., Němec et al., 2018). The plot indicates that there are two main wave populations of different wave normal angles. At lower L -shells ($L \sim 4$), primarily large ($>60^\circ$) wave normal angles are observed. On the other hand, primarily low ($<30^\circ$) wave normal angles are observed at larger L -shells (≥ 5).

In order to further investigate the wave propagation from the equatorial plane at larger distances to the Kannuslehto station, we perform a ray tracing analysis for a selected event. For this purpose, a QP event observed on 20 November 2017 at frequencies around 2 kHz, already shown in Figure 1b, was chosen. The zoomed frequency-time spectrogram of this event is shown in Figure 9. The event measurements obtained by Kannuslehto, RBSP A, and RBSP B are depicted in Figures 9a–9c, respectively. It can be seen that while the Kannuslehto station observed the event continuously between around 2:30 and 6:30 UT, individual spacecraft detected the event only for limited time intervals, marked by the vertical white dashed lines. This is because the event detection is controlled not only by the event duration, but also by the spacecraft location (see further). Although the event is comparatively weak, compared to the strongest spacecraft emissions depicted, the quasiperiodic modulation of the event intensity (better visible in even more zoomed view, not shown) provides a confirmation that this is indeed the same event observed by the spacecraft and the Kannuslehto station. We note that another event occurring at around 1 kHz is more or less visible by all instruments, but it will not be analyzed further.

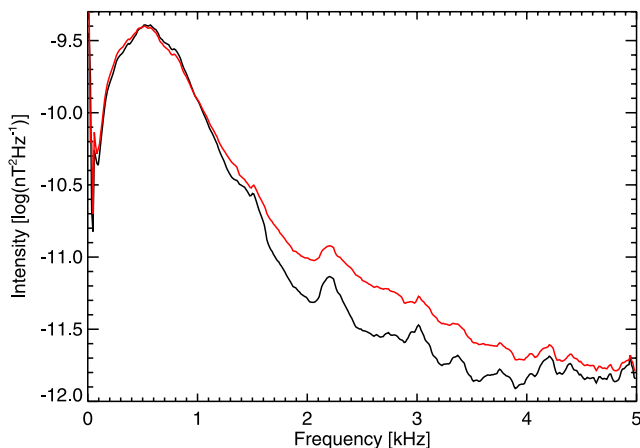


Figure 6. Average frequency spectrum measured by the Kannuslehto station in the frequency range between 0 and 5 kHz during all the analyzed campaigns (black curve) and during the times of the events (red curve).

The spacecraft locations in solar magnetic (SM) coordinates during the time interval corresponding to Figure 9 are shown in Figure 10. The positions of RBSP A and RBSP B are drawn by the red and blue curves, respectively. Positions of the spacecraft during their detections of the event, as marked by the dashed white lines in Figure 9, are shown by the thick curves. The red and blue curves near the Earth's surface in Figure 10a correspond to the MLT interval of the event as observed by RBSP A and RBSP B, respectively. Moreover, MLTs of the Kannuslehto station at the times of the event are depicted by the violet curve on the Earth's surface.

Results of the backward ray tracing analysis of the waves forming the event are depicted in Figure 10b. A ray tracing code assuming a dipole magnetic field model (e.g., Němec et al., 2021; Santolík et al., 2016) was used for this analysis. The density model assumes a diffusive equilibrium with the following parameters: reference altitude 1,000 km; electron temperature 1,700 K; plasma number density at the reference altitude $4,000 \text{ cm}^{-3}$; relative abundance of oxygen ions 55%, hydrogen ions 40%, and helium ions 5%. We opt to start the waves at the bottom of the ionosphere ($\sim 150 \text{ km}$) with vertical wave normals and thus attempt to backward reconstruct the trajectory of the waves that might have eventually made it to the ground. Given the possibility

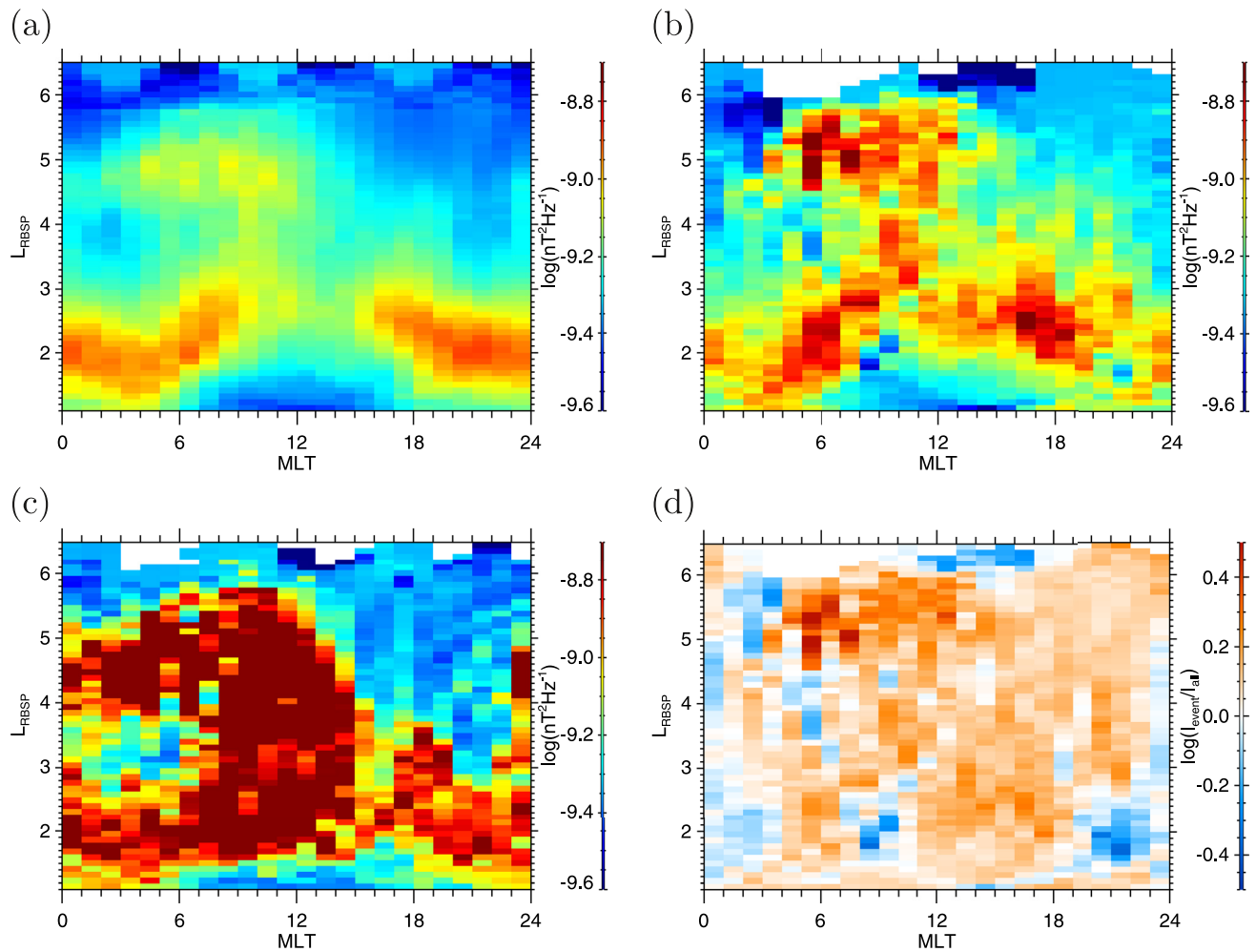


Figure 7. (a) Average power spectral density of magnetic field fluctuations in the frequency range between 2 and 4 kHz measured by RBSP A as a function of MLT and L -shell. (b) Same as (a), but only intensities measured during the times of the events at the Kannuslehto station were considered. (c) Same as (a), but only for intensities when Kp index value was larger than 5. (d) Logarithm of ratio of intensities shown in panels (b) and (a).

of the wave propagation in the Earth-ionosphere waveguide, we do not start the waves necessarily exactly from the Kannuslehto location (marked by the cross in Figure 10b), but rather from a range of geomagnetic latitudes (40° – 55°). We also note that as all the observations took place in not too different longitudes, we limit the analysis to a single magnetic meridian. The calculated wave trajectories are shown by the purple curves in Figure 10b. The black curves correspond to the dipole magnetic field lines at $L = 3, 4, \text{ and } 5$, respectively. It can be seen that although all the plotted wave trajectories start southwards from Kannuslehto, they eventually cross the RBSP orbits during the event and may thus explain the observations. Specifically, the initial geomagnetic latitudes of these wave trajectories in Figure 10b are $42^\circ, 45^\circ, 48^\circ, 51^\circ, \text{ and } 53.7^\circ$, while the Kannuslehto geomagnetic latitude is around 64.5° . Such a propagation scheme thus requires a considerable ($\sim 1,800$ km) propagation in the Earth-ionosphere waveguide upon exiting the ionosphere. Note that the QP events arrive to Kannuslehto mostly from south based on the analysis (not shown). The calculated wave normal angles upon the arrival to the RBSP spacecraft orbits are about 60° . The actual wave normal angle values based on the RBSP wave measurements are mostly within about 30° , consistent with the statistical results in Figure 8. This means that the majority of the waves observed by RBSP cannot propagate to the ground unducted.

4. Discussion

Based on our results, one can discuss the type of emissions typically observed at Kannuslehto. The analyzed emissions are observed over a rather broad MLT interval ranging from dawn to dusk, with peak occurrence

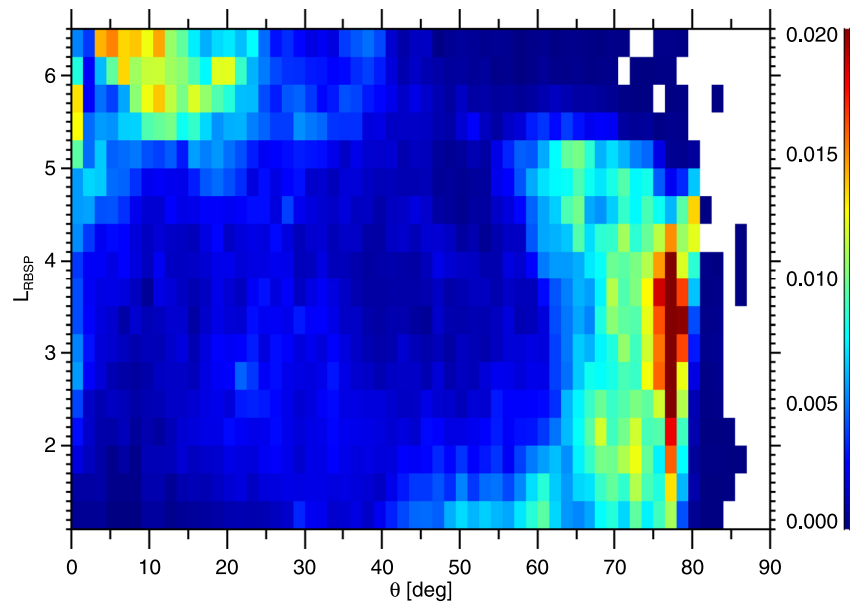


Figure 8. Color-coded probability density of the wave normal angle measured by RBSP in the frequency range between 2 and 4 kHz as a function of L -shell measured during the times of the events.

shortly before noon. This is in agreement with average Kannuslehto intensity profiles. It is generally difficult to distinguish individual events on the nightside, which is dominated by lightning generated emissions. Apart from these nightside emissions, the events analyzed in the present study are among the most significant waves observed at Kannuslehto. The results obtained are thus of a global importance for the whistler mode wave propagation to a subauroral ground-based station.

The events detected by Kannuslehto typically last for several hours. However, they are often observed for several consecutive days. This can be most likely explained by the actual duration being up to a few days, but spatially confined to central MLTs. As the Kannuslehto station rotates along with the Earth, it then periodically gets in and out of the event, explaining its apparently limited MLT extent and the tendency to occur during several consecutive days.

The comparison of intensity distribution measured by RBSP during the event detections with the long-term average situation reveals that the most significant intensity maximum, likely corresponding to the emissions observed on the ground, occurs at L -shells between about 5 and about 6 in the morning hours, being attributed to dawn side chorus. We note, in this regard, that the L -shell of the Kannuslehto station is about 5.5.

The backward ray tracing analysis further revealed wave normal angles of equatorial waves at given L -shells needed for the emissions to propagate to the ground. It turns out that the respective wave normal angles close to the equatorial plane need to be quite large, around 60° . The wave normal angles actually observed by RBSP, both during the analyzed event and globally at given L -shells and MLTs, are much lower. Assuming unducted propagation, only the waves with beyond typical wave normal angles are thus eventually detectable by Kannuslehto. This indicates that only a small fraction of unducted waves makes it from the equatorial large L -shell region down to the ground. Such waves would correspond to the very edge of the real wave normal angle distribution, which cannot be, however, experimentally determined. Moreover, the Earth-ionosphere waveguide propagation apparently needs to be involved for the waves to be detectable by a high latitude station like Kannuslehto. Another scenario allowing the wave to get to the ground is ducted propagation (Demekhov et al., 2020). Such a propagation may or may not be followed by a propagation in the Earth-ionosphere waveguide and would allow the wave to seamlessly reach Kannuslehto. The intensity of the analyzed event observed by Kannuslehto is comparable to the intensity of the event analyzed by Demekhov et al. (2020). Assuming a similar source intensity, and taking into account that only a small part of the waves can make it to the ground unducted, the ducted propagation scenario seems to be more likely.

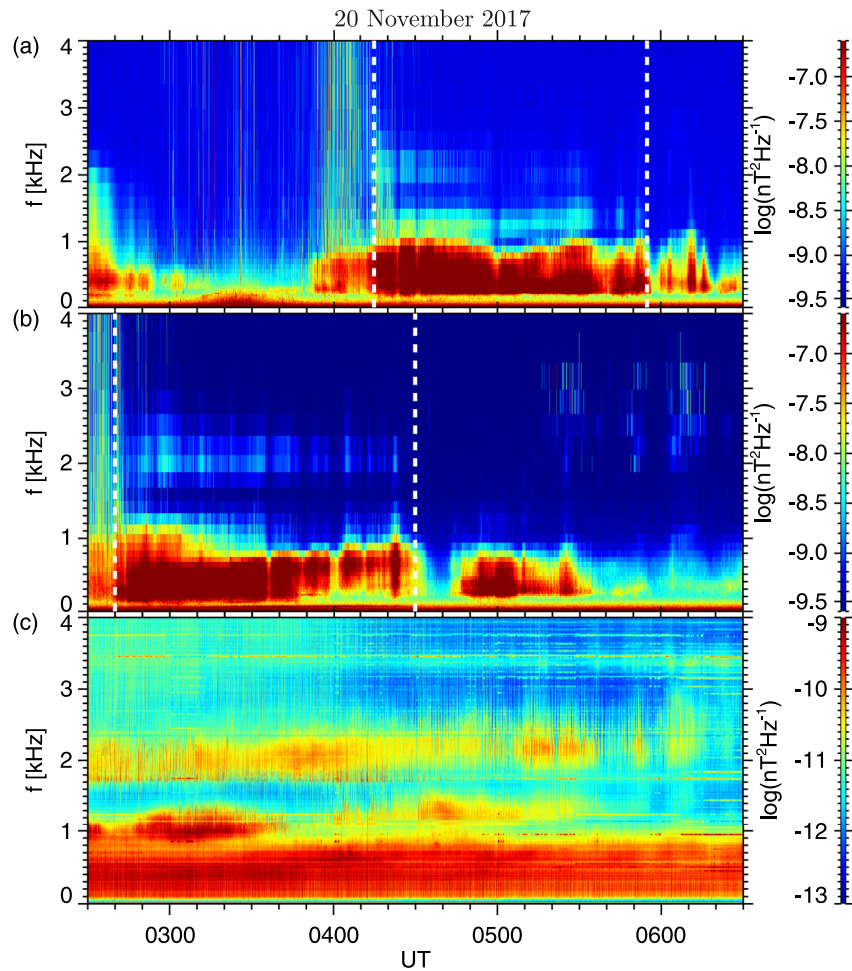


Figure 9. Zoomed spectrograms of the event observed on 20 November 2017 (shown in Figure 1b) at frequencies around 2 kHz as measured by (a) RBSP A, (b) RBSP B, and (c) the Kannuslehto station. The white dashed lines show the interval of the event detection by the individual spacecraft.

Note that both the suggested propagation schemes may naturally explain why some of the emissions detected at Kannuslehto have frequencies larger than the equatorial electron cyclotron frequency at a given L -shell (Manninen et al., 2021; Martinez-Calderon, Manninen, et al., 2021). They simply originate at lower equatorial L -shells propagate either ducted or unducted to the bottom of the ionosphere, and only get to larger L -shells during their propagation in the Earth-ionosphere waveguide, in line with the event considered by Titova et al. (2017).

5. Conclusions

An analysis of the events characterized by a significant intensity enhancement at frequencies between about 1.5 and 4 kHz in the Kannuslehto measurements was performed. Altogether, 465 events were found between December 2012 and October 2019. The events typically occur on the dawn side during periods of increased geomagnetic activity, and they typically last for a few hours. Frequent event observations during several consecutive days indicate that they may be actually quite long-lasting, with the observed Kannuslehto event durations being shorter due to the event limited azimuthal extents.

A comparison of intensity measurements performed by the RBSP spacecraft during the times of the events and with their long-term average revealed the MLT– L -shell interval with significant intensity enhancement during the events, corresponding likely to the dawn-side chorus.

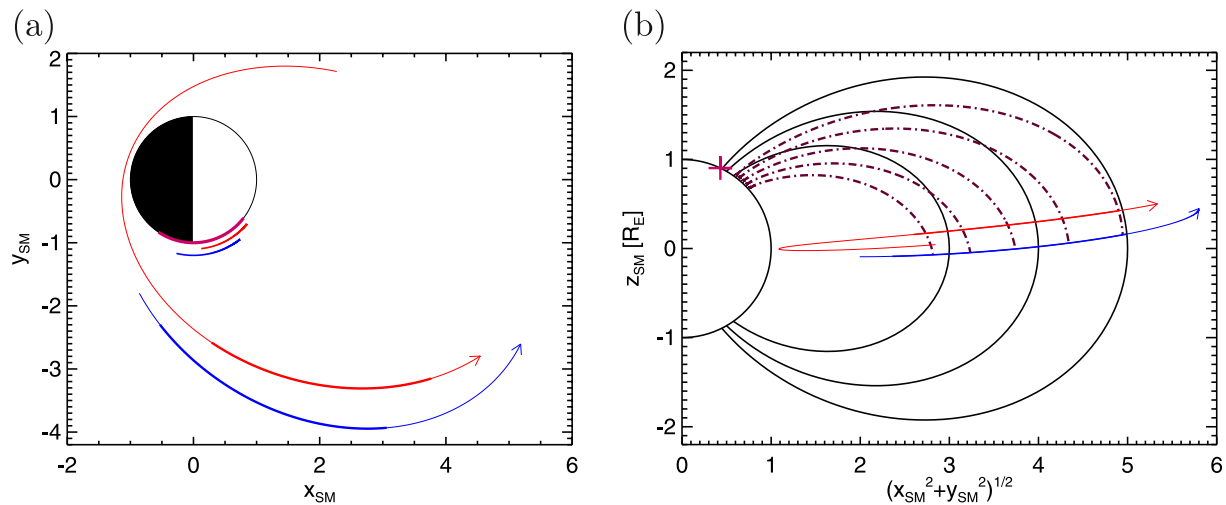


Figure 10. (a) Spacecraft positions during the detection of the whole event by RBSP A (red curve) and RBSP B (blue curve). The thick parts of the curves show the positions of the spacecraft during their observations of the event as drawn by white lines in Figure 9. The violet curve shows the location of the Kannuslehto station during the observed event. The red and blue curves near the Earth indicate MLT values during the spacecraft event measurements. (b) Ray tracing of the waves possibly observed at the RBSP spacecraft from the Earth surface. The red and blue curves have the same meaning as in panel (a). Position of the Kannuslehto station is denoted by the violet cross. The dipole field lines are denoted by the black curves.

We further performed a backward ray tracing analysis for a selected event observed by both RBSP spacecraft. The results indicate that the RBSP spacecraft located in the equatorial plane at L -shells comparable with the Kannuslehto station position can in principle detect the same emissions as Kannuslehto, although it is a rather small fraction of all emissions detected at the spacecraft. Specifically, assuming unducted propagation, only the waves with comparatively large wave normal angles ($\sim 60^\circ$) in the equatorial region are likely to propagate through the ionosphere to the ground. Additionally, the wave propagation in the Earth-ionosphere waveguide seems to be needed for the waves to propagate to a high-latitude station like Kannuslehto. Another possible scenario involves wave ducting. This allows for a seamless wave propagation from the equatorial region to the ground, eventually again followed by the propagation in the Earth-ionosphere waveguide. Both the suggested propagation schemes may explain the occasional wave emissions with frequencies larger than the equatorial cyclotron frequency measured by Kannuslehto (Manninen et al., 2021).

Data Availability Statement

The Van Allen Probes data used in this paper can be accessed from <https://emfisis.physics.uiowa.edu/Flight/RBSP-A/L2> and <https://emfisis.physics.uiowa.edu/Flight/RBSP-B/L2> (EMFISIS wave data). The filtered VLF Kannuslehto data are available at https://www.sgo.fi/pub_vlf/ as the power spectrograms in 24-hr, 1-hr, and 1-min intervals for all campaigns 2006–2022.

Acknowledgments

The authors acknowledge the support of GACR Grant 21-01813S.

References

- Aryan, H., Bortnik, J., Meredith, N. P., Horne, R. B., Sibeck, D. G., & Balikhin, M. A. (2021). Multi-parameter chorus and plasmaspheric hiss wave models. *Journal of Geophysical Research: Space Physics*, 126(1), e2020JA028403. <https://doi.org/10.1029/2020JA028403>
- Bespalov, P. A., Parrot, M., & Manninen, J. (2010). Short-period VLF emissions as solitary envelope waves in a magnetospheric plasma maser. *Journal of Atmospheric and Solar-Terrestrial Physics*, 72(17), 1275–1281. <https://doi.org/10.1016/j.jastp.2010.09.001>
- Bezděková, B., Němec, F., Manninen, J., Hospodarsky, G. B., Santolík, O., Kurth, W. S., & Hartley, D. P. (2020). Conjugate observations of quasiperiodic emissions by the Van Allen Probes spacecraft and ground-based station Kannuslehto. *Journal of Geophysical Research: Space Physics*, 125(6), e2020JA027793. <https://doi.org/10.1029/2020JA027793>
- Bezděková, B., Němec, F., Parrot, M., Hajoš, N., Záhřava, J., & Santolík, O. (2019). Dependence of properties of magnetospheric line radiation and quasiperiodic emissions on solar wind parameters and geomagnetic activity. *Journal of Geophysical Research: Space Physics*, 124(4), 2552–2568. <https://doi.org/10.1029/2018JA026378>
- Breuilhard, H., Agapitov, O., Artemyev, A., Krasnoselskikh, V., Contel, O. L., Cully, C. M., et al. (2014). On the origin of falling-tone chorus elements in Earth's inner magnetosphere. *Annales Geophysicae*, 32(12), 1477–1485. <https://doi.org/10.5194/angeo-32-1477-2014>
- Budden, K. G. (1961). *The wave-guide mode theory of wave propagation*. Logos Press.
- Carson, W. B., Koch, J. A., Pope, J. H., & Gallet, R. M. (1965). Long period very low frequency emission pulsations. *Journal of Geophysical Research*, 70(17), 4293–4303. <https://doi.org/10.1029/JZ070i017p04293>

- Cohen, M. B., Lehtinen, N. G., & Inan, U. S. (2012). Models of ionospheric VLF absorption of powerful ground based transmitters. *Geophysical Research Letters*, 39(24), L24101. <https://doi.org/10.1029/2012GL054437>
- Demekhov, A. G., Manninen, J., Santolík, O., & Titova, E. E. (2017). Conjugate ground-spacecraft observations of VLF chorus elements. *Geophysical Research Letters*, 44(23), 11–735. <https://doi.org/10.1002/2017GL076139>
- Demekhov, A. G., Titova, E. E., Manninen, J., Nikitenko, A. S., & Pilgaev, S. V. (2021). Short periodic VLF emissions observed simultaneously by Van Allen Probes and on the ground. *Geophysical Research Letters*, 48(20), e2021GL095476. <https://doi.org/10.1029/2021GL095476>
- Demekhov, A. G., Titova, E. E., Manninen, J., Pasmanik, D. L., Lubchich, A. A., Santolík, O., et al. (2020). Localization of the source of quasi-periodic VLF emissions in the magnetosphere by using simultaneous ground and space observations: A case study. *Journal of Geophysical Research: Space Physics*, 125(5), e2020JA027776. <https://doi.org/10.1029/2020JA027776>
- Graf, K. L., Lehtinen, N. G., Spasojevic, M., Cohen, M. B., Marshall, R. A., & Inan, U. S. (2013). Analysis of experimentally validated trans-ionospheric attenuation estimates of VLF signals. *Journal of Geophysical Research: Space Physics*, 118(5), 2708–2720. <https://doi.org/10.1002/jgra.50228>
- Green, J. L., Boardsen, S., Garcia, L., Taylor, W. W. L., Fung, S. F., & Reinisch, B. W. (2005). On the origin of whistler mode radiation in the plasmasphere. *Journal of Geophysical Research*, 110(A3), A03201. <https://doi.org/10.1029/2004JA010495>
- Helliwell, R. A. (1965). *Whistlers and related ionospheric phenomena*. Stanford University Press.
- Jaynes, A. N., Lessard, M. R., Takahashi, K., Ali, A. F., Malaspina, D. M., Michell, R. G., et al. (2015). Correlated Pc4–5 ULF waves, whistler-mode chorus, and pulsating aurora observed by the Van Allen Probes and ground-based systems. *Journal of Geophysical Research: Space Physics*, 120(10), 8749–8761. <https://doi.org/10.1002/2015JA021380>
- Kletzing, C. A., Kurth, W. S., Acuna, M., MacDowall, R. J., Torbert, R. B., Averkamp, T., et al. (2013). The electric and magnetic field instrument suite and integrated science (EMFISIS) on RBSP. *Space Science Reviews*, 179(1–4), 127–181. <https://doi.org/10.1007/s11214-013-9993-6>
- Li, W., Thorne, R. M., Bortnik, J., Shprits, Y. Y., Nishimura, Y., Angelopoulos, V., et al. (2011). Typical properties of rising and falling tone chorus waves. *Geophysical Research Letters*, 38(14), L14103. <https://doi.org/10.1029/2011GL047925>
- Ma, Q., Mourenas, D., Li, W., Artemyev, A., & Thorne, R. M. (2017). VLF waves from ground-based transmitters observed by the Van Allen Probes: Statistical model and effects on plasmaspheric electrons. *Geophysical Research Letters*, 44(13), 6483–6491. <https://doi.org/10.1002/2017GL073885>
- Manninen, J. (2005). *Some aspects of ELF-VLF emissions in geophysical research* (pp. 53–84–85–110). Sodankylä Geophysical Observatory Publications. Retrieved from <https://www.sgo.fi/Publications/SGO/thesis/ManninenJyrki.pdf>
- Manninen, J., Kleimenova, N., Martinez-Calderon, C., Gromova, L., & Turunen, T. (2022). Unexpected VLF bursty-patches above 5 kHz: A review of long-duration VLF series observed at Kannuslehto, Northern Finland. *Surveys in Geophysics*, 1–27. <https://doi.org/10.1007/s10712-022-09741-0>
- Manninen, J., Kleimenova, N., Turunen, T., Nikitenko, A., Gromova, L., & Fedorenko, Y. (2021). New type of short high-frequency VLF patches (“VLF birds”) above 4–5 kHz. *Journal of Geophysical Research: Space Physics*, 126(4), e2020JA028601. <https://doi.org/10.1029/2020JA028601>
- Martinez-Calderon, C., Katoh, Y., Manninen, J., Kasahara, Y., Matsuda, S., Kumamoto, A., et al. (2020). Conjugate observations of dayside and nightside VLF chorus and QP emissions between Arase (ERG) and Kannuslehto, Finland. *Journal of Geophysical Research: Space Physics*, 125(1), e2019JA026663. <https://doi.org/10.1029/2019JA026663>
- Martinez-Calderon, C., Katoh, Y., Manninen, J., Santolík, O., Kasahara, Y., Matsuda, S., et al. (2021). Multievent study of characteristics and propagation of naturally occurring ELF/VLF waves using high-latitude ground observations and conjunctions with the Arase satellite. *Journal of Geophysical Research: Space Physics*, 126(2), e2020JA028682. <https://doi.org/10.1029/2020JA028682>
- Martinez-Calderon, C., Manninen, J. K., Manninen, J. T., & Turunen, T. (2021). A review of unusual VLF bursty-patches observed in Northern Finland for Earth, Planets and Space. *Earth Planets and Space*, 73(1), 1–14. <https://doi.org/10.1186/s40623-021-01516-y>
- Martinez-Calderon, C., Němec, F., Katoh, Y., Shiokawa, K., Kletzing, C., Hospodarsky, G., et al. (2020). Spatial extent of quasi-periodic emissions simultaneously observed by Arase and Van Allen Probes on 29 November 2018. *Journal of Geophysical Research: Space Physics*, 125(9), e2020JA028126. <https://doi.org/10.1029/2020JA028126>
- Martinez-Calderon, C., Shiokawa, K., Miyoshi, Y., Keika, K., Ozaki, M., Schofield, I., et al. (2016). ELF/VLF wave propagation at subauroral latitudes: Conjugate observation between the ground and Van Allen Probes A. *Journal of Geophysical Research: Space Physics*, 121(6), 5384–5393. <https://doi.org/10.1002/2015JA022264>
- Menk, F. W. (2011). Magnetospheric ULF waves: A review. In W. Liu & M. Fujimoto (Eds.), *The dynamic magnetosphere* (pp. 223–256). Springer Netherlands. https://doi.org/10.1007/978-94-007-0501-2_13
- Němec, F., Bezděková, B., Manninen, J., Parrot, M., Santolík, O., Hayosh, M., & Turunen, T. (2016). Conjugate observations of a remarkable quasi-periodic event by the low-altitude DEMETER spacecraft and ground-based instruments. *Journal of Geophysical Research: Space Physics*, 121(9), 8790–8803. <https://doi.org/10.1002/2016JA022968>
- Němec, F., Hospodarsky, G. B., Bezděková, B., Demekhov, A. G., Pasmanik, D. L., Santolík, O., et al. (2018). Quasi-periodic whistler mode emissions observed by the Van Allen Probes spacecraft. *Journal of Geophysical Research: Space Physics*, 123(11), 8969–8982. <https://doi.org/10.1029/2018JA026058>
- Němec, F., Santolík, O., & Parrot, M. (2021). Doppler shifted Alpha transmitter signals in the conjugate hemisphere: DEMETER spacecraft observations and raytracing modeling. *Journal of Geophysical Research: Space Physics*, 126(4), e2020JA029017. <https://doi.org/10.1029/2020JA029017>
- Němec, F., Santolík, O., Parrot, M., & Rodger, C. J. (2010). Relationship between median intensities of electromagnetic emissions in the VLF range and lightning activity. *Journal of Geophysical Research*, 115(A8). <https://doi.org/10.1029/2010JA015296>
- Rodger, C. J., Clilverd, M. A., Yearby, K., & Smith, A. J. (2000). Is magnetospheric line radiation man-made? *Journal of Geophysical Research*, 105(A7), 15981–15990. <https://doi.org/10.1029/1999JA000413>
- Santolík, O., Parrot, M., Inan, U. S., Burešová, D., Gurnett, D. A., & Chum, J. (2009). Propagation of unducted whistlers from their source lighting: A case study. *Journal of Geophysical Research*, 114(A3), A03212. <https://doi.org/10.1029/2008JA013776>
- Santolík, O., Parrot, M., & Lefeuvre, F. (2003). Singular value decomposition methods for wave propagation analysis. *Radio Science*, 38(1), 1010. <https://doi.org/10.1029/2000RS002523>
- Santolík, O., Parrot, M., & Němec, F. (2016). Propagation of equatorial noise to low altitudes: Decoupling from the magnetosonic mode. *Geophysical Research Letters*, 43(13), 6694–6704. <https://doi.org/10.1002/2016GL069582>
- Santolík, O., Pickett, J. S., Gurnett, D. A., Menietti, J. D., Tsurutani, B. T., & Verkhoglyadova, O. (2010). Survey of Poynting flux of whistler mode chorus in the outer zone. *Journal of Geophysical Research*, 115(A7), A00F13. <https://doi.org/10.1029/2009JA014925>
- Santolík, O., Pickett, J. S., Gurnett, D. A., & Storey, L. R. O. (2002). Magnetic component of narrowband ion cyclotron waves in the auroral zone. *Journal of Geophysical Research*, 107(A12), SMP 17–1–SMP 17–14. <https://doi.org/10.1029/2001JA000146>

- Sato, N., & Kokubun, S. (1980). Interaction between ELF-VLF emissions and magnetic pulsations: Quasiperiodic ELF-VLF emissions associated with Pc 3–4 magnetic pulsations and their geomagnetic conjugacy. *Journal of Geophysical Research*, 85(A1), 101–113. <https://doi.org/10.1029/JA085iA01p00101>
- Sonwalkar, V. S. (1995). *Handbook of atmospheric electrodynamics. Chapter Magnetospheric LF-, VLF-, and ELF-Waves* (Vol. 2). CRC Press.
- Titova, E. E., Demekhov, A. G., Manninen, J., Pasmanik, D. L., & Larchenko, A. V. (2017). Localization of the sources of narrow-band noise VLF emissions in the range 4–10 kHz from simultaneous ground-based and Van Allen Probes satellite observations. *Geomagnetism and Aeronomy*, 57(6), 706–718. <https://doi.org/10.1134/S0016793217060135>
- Titova, E. E., Kozelov, B. V., Demekhov, A. G., Manninen, J., Santolík, O., Kletzing, C. A., & Reeves, G. (2015). Identification of the source of quasiperiodic VLF emissions using ground-based and Van Allen Probes satellite observations. *Geophysical Research Letters*, 42(15), 6137–6145. <https://doi.org/10.1002/2015GL064911>
- Trakhtengerts, V. Y., & Rycroft, M. J. (2008). *Whistler and Alfvén mode cyclotron masers in space. Cambridge Atmospheric and Space Sciences Series*. Cambridge University Press.
- Záhlava, J., Němec, F., Santolík, O., Kolmašová, I., Hospodarsky, G. B., Parrot, M., et al. (2018). Longitudinal dependence of whistler mode electromagnetic waves in the Earth's inner magnetosphere. *Journal of Geophysical Research: Space Physics*, 123(8), 6562–6575. <https://doi.org/10.1029/2018JA025284>
- Záhlava, J., Němec, F., Santolík, O., Kolmašová, I., Hospodarsky, G. B., Parrot, M., et al. (2019). Lightning contribution to overall whistler mode wave intensities in the plasmasphere. *Geophysical Research Letters*, 46(15), 8607–8616. <https://doi.org/10.1029/2019GL083918>